SSC20-VII-04

DEBRIS - A Small Satellite Approach to Active Debris Removal

Niklas Wendel
German Network of Young Scientists - juFORUM e.V.
Zu den Wiesen 12, 51147 Cologne, Germany
niklas.wendel@juforum.de

Tilman Hoffbauer
German Network of Young Scientists - juFORUM e.V.
tilman.hoffbauer@juforum.de

Louisa Gerhard
German Network of Young Scientists - juFORUM e.V.
louisa.gerhard@juforum.de

ABSTRACT

The current space debris situation is distressing and becomes even worse with the launch of many new satellites and the emerging trend of mega-constellations. While efforts are made to implement a mechanism for deorbiting into newly launched satellites, these mechanisms can fail and old satellites may not even have it. By collision of these large objects, many new smaller objects are generated which in turn may generate new collisions. This effect known as the Kessler syndrome will lead to an endangering of all future spaceflight if no solution is found. The DEBRIS project wants to deorbit large objects from LEO to remove their collision risk. As conventional propulsion is expensive for the deorbit of many objects, drag sails and electrodynamic tethers to harvest the necessary energy in orbit. An additional reduction of fuel consumption is achieved by a special near-approach flight strategy. To ensure a versatile and reliant capturing while preserving low mass a novel capturing mechanism is proposed. Using these techniques, the DEBRIS probe can be designed as a small satellite. This allows for a great reduction of mass, volume, and thus costs, making the removal of many large objects affordable.

The Distressing Space Debris Situation

Even though the immense danger a self-enforcing collision of debris in LEO poses to all current and future, manned and unmanned, scientific and commercial spaceflight has been heavily discussed since it emerged in the scientific awareness in 1978,[1] a technical solution to deorbit existing space debris and thus lower the risk of a chain reaction of collisions has not been found and successfully demonstrated yet. Especially larger debris parts like inoperative satellites can easily become a source of exponentially more space debris if they collide, which is why it is important to remove these objects from orbit before the start an unstoppable chain reaction. Already in 1991, Donald Kessler states that "[...] actions must begin now in order to be effective. [...] That engineering development should begin now, since there is little uncertainty that it will be required."[2] Of course, the awareness of the space debris problem rose in the last years and it has been the subject of many research projects to find suitable solutions. Many of those solutions aim at making sure that spacecraft sent into orbit now will eventually deorbit themselves at the end of their lifespan[3] or implementing collision warn and avoidance systems.[4] Those strategies should undoubtedly be further enhanced. At the same time, a working mechanism for debris removal is inevitable for the successful mastery of the space flight crisis we will face if the problem is not tackled.

One of the most important tasks to solve to create a working active removal system is the target capturing. Many possible solutions have been considered in the past, but none has been strikingly safe and efficient at the same time. Another main problem active debris removal poses is the high amount (and the closely linked high mission costs) of conventional propellant needed to create enough momentum to deorbit debris objects. As a solution, a combination of passive deorbit technologies is proposed: Momentum will be created using a drag sail and an electrodynamic tether connected to the DEBRIS

probe. The current-carrying tether will be ejected pointing in earth direction, therefore perpendicular standing in earth's magnetic field and allowing the Lorentz force to alter the direction of the DEBRIS probe's orbit.

Suitability of Large Debris Objects Deorbiting Using Drag Sail and Tether

Distribution and Properties of Large Debris Objects

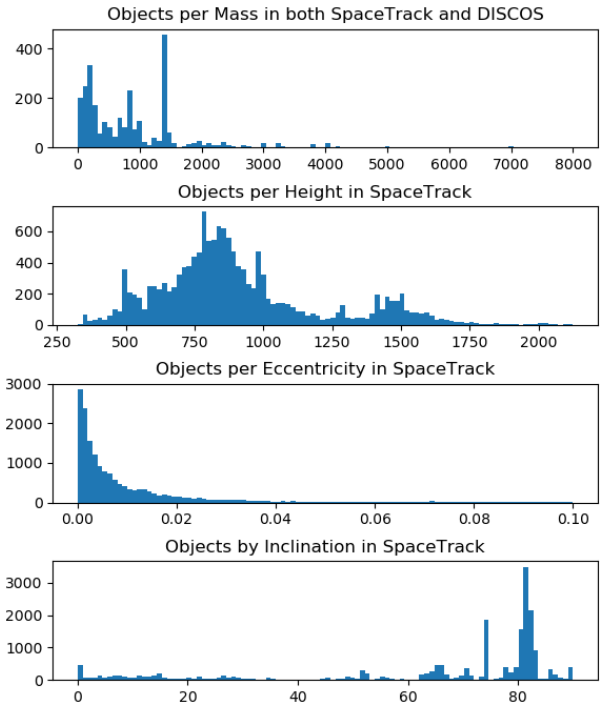

Figure 1: Space objects in LEO plotted over mass, height, eccentricity and inclination

To evaluate the suitability of sail and tether for the deorbiting of large objects, the number, properties, and distribution of these objects must be known. Fortunately, there are several databases available which track space objects not too small for measurement.[5,6] For this publication, both cited databases were fetched and merged using the NORAD ID, an international identifier for objects in space. Whereas SATCAT contains detailed orbital data, DISCOS provides information on the mass of the object - a crucial value for the calculation of deorbiting times. The data was filtered to only contain not yet decayed objects. This way, a total of 19451 objects were found. 14708 of these objects contain orbit data with 2803 objects additionally having mass information. The ISS was manually removed from the data.

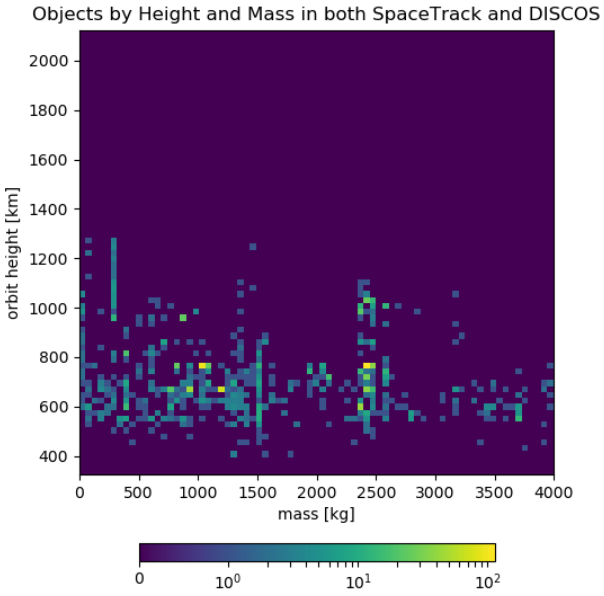

Figure 2: Space objects in LEO as a heatmap over mass and height

Figure 1 shows different plots of the acquired data. The plots only contain objects in LEO (height $\leq$ 2125km) and with a minimum mass of 50kg. Calculating the percentiles shows that 85% of the objects have a mass of less than 1434kg, a height of less than 1408km and an eccentricity of less than 0.086. Further investigation of the data shows that there are 24 objects with a mass greater than 8000kg totaling a mass of 203295kg. These objects do not appear in the plot. With respect to the inclination three hotspots at 0°, 65°, 75° and most notably 82° can be observed. The heatmap in Figure 2 shows a non-uniform distribution of the objects regarding height and mass. It can be observed that there are some hotspots with a lot of objects in a similar configuration. There seems to be no relation between object mass and orbital height.

Simulation of Drag Sail and Tether

Since its deorbiting devices can be regarded as the payload of the DEBRIS probe, an initial definition of a meaningful payload envelope is necessary to design the adequate satellite bus. To gain meaningful insights for the performance of possible deorbiting configurations, a numerical simulation tool has been developed. Calculations for atmospheric and electromagnetic forces have been conducted, using advanced Newtonian theory combined with the properties of the extrapolated standard atmosphere and a numerical representation of the tether.[7] To verify the compliance with other numerical models, the simulation has been validated against results

from another mission.[8] A tether is more efficient on greater orbit heights, while a drag sail excels on lower orbit heights. Thus the available payload mass must be distributed over both mechanisms. Therefore a set of configurations were derived for some manually chosen payload masses. To determine the performance of these, the previously described subset of debris objects has been evaluated as reference data for all deorbiting simulations. To add evaluation criteria, the performance of the configurations has also been evaluated for a defined list of high-risk objects. The evaluation of predefined configurations leads to the selection of a combination of 40m^2 sail area and a tether length of 300 meters. The estimated average deorbit time for all considered debris objects and this configuration is 437 days. Even though a configuration with a large tether leads to slightly lower deorbit times around 400 days, the described configuration is preferred. This is justified by a large difference in the deorbit time's standard deviation, which is a factor of more than 300 higher for configurations with large tethers. During the ongoing development of the probe fine adjustments of these parameters remain possible.

The DEBRIS Mission

System layout and mission envelope

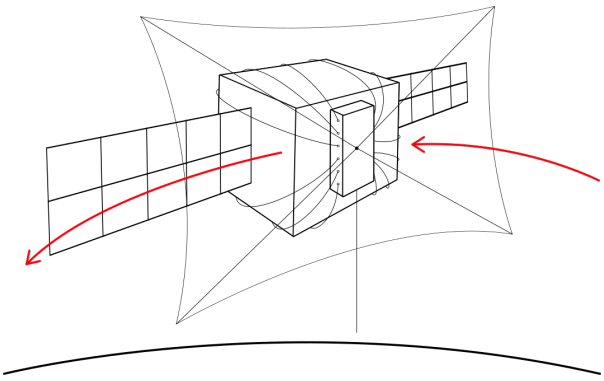

Figure 3: Debris probe after capturing of target, spatial orientation of electrodynamic tether, sail and probe relative to target, earth and orbit

The DEBRIS probe consists of several subsystems which will enable the active removal of a chosen target. Crucial for mission success is the controllable capturing of the target. The capturing system is an arrangement of electromagnets or pressurized gas chambers that shoot small permanent magnets in the direction of the target. Those magnets are connected to DEBRIS using aramid ropes, thus establishing a permanent connection of target and probe once the magnets connect behind the target. The flight path of the magnetic projectiles will be controlled using electromagnetic coils, two of which are located at each side surface of the DEBRIS probe. Between each pair of coils, up to three permanent magnets can be placed resulting in a total of 12 magnets that can be shot. The localization, exact measuring, and constant monitoring of the target are essential conditions to perform a safe capturing, which is why the remote sensing subsystem needs to be able to fulfill these different tasks. The first information about the target, mainly the current distance from target to probe, will be collected using two RADAR sensors. For close-up measuring of the target, a solid-state LIDAR will be used in combination with cameras. An onboard computer will collect and process the sensor information. While sending some of this information to the ground station to enable control over the mission, the information needed for time crucial decisions like capturing success will be processed and used directly. The power supply for all subsystems is ensured through solar panels, located mostly at the target opposing side, but also at all other free areas. The solar panels are designed and arranged in a way that enables a failure mode in which the DEBRIS probe can be supplied with enough energy to prevent system damage independent of its position towards the sun. That way, system recovery can be guaranteed even if the AOCS fails. Since the DEBRIS probe will be taken into an orbit with a predefined height by a carrier rocket, the probe will have to be able to fly into the exact orbit of the target with its own propulsion (orbit transfer). When the target orbit is reached, relative maneuvering to get close enough for capturing has to be conducted (relative navigation). These two different kinds of movement have to be performed by different thrusters. In the context of relative navigation, the DEBRIS probe will also have to countervail the self-rotation of the target. Movement information will be collected by the attitude and orbit control system (AOCS) and remote sensing. Once the target has been captured, the momentum necessary for deorbit is generated via an electrodynamic tether, using the resulting Lorentz force, and via a drag sail, using atmospheric drag. The electrodynamic tether is located at a side surface and deployed pointing towards earth. The drag sail is stowed in an openable compartment at the target opposing side and is unfolded orthogonally to use as much atmospheric friction as possible. The DEBRIS probe will also feature several experimental slots. Those slots offer the pos-

sibility to fly experimental system components and collect information about their flight qualification.

Considering the current design status, the DEBRIS probe will weigh an expected 40 kg and fit in $\frac{1}{5}$ of an EELV Secondary Payload Adapter (ESPA) slot. This way, five DEBRIS probes can share one ESPA slot in the future and each deorbit a different target. After being set into orbit by the carrier rocket at a minimum of 350 km orbit height, the DEBRIS probe will be able to fly to orbit heights in the magnitude of 2000 km, making sure that space debris pieces in these heavily used and therefore high-risk orbits can be reached by the probe. As said before, after the general target orbit has been reached, the relative maneuvering has to be performed to get close enough to the target to start the capturing mechanism. After the target has been captured and the DEBRIS probe is permanently connected with it, the self-rotation of the target has to be balanced to perform a safe and controlled deorbit. Propellant usage is calculated taking an extensive margin into account. The propellant that has not been used for navigation and maneuvering after the successful capturing can be utilized to increase the eccentricity of the flown orbit. Since the perigee of the orbit will be close to the earth and deeper in its atmosphere, the drag sail of the DEBRIS probe can be used more efficiently after an eccentricity increase.

Mission phases and flight planning

The mission operation and flight planning of the proposed mission is characterized by strong differences between a total of five mission phases at three different stages. The mission phases can be chronologically sorted into launch and early operations (LEOP), far approach, near approach, capturing, and deorbiting. The mentioned mission stages are mission start consisting of LEOP and far approach, dynamic close proximity operations consisting of the near approach and capturing, and the deorbit itself.

After the launch on a rideshare opportunity and orbit injection, system checkout and stabilization is performed in LEOP. The following phase of the far approach can be compared to the approach to a reserved orbital box which includes the target of the mission. This is the transition to the dynamic mission phase, which is done by switching from far to near approach. During this, the coordinate system used for navigation is switched from absolute (e.g. ECEF) to relative to the local orbital frame (LOF) with its center at the target.

The size of the target box and the proximity maneuvers are defined by uncertainties concerning probe and target locations and trajectories. The ranging by ground radars has an inaccuracy of up to +/- 2000 meters.[9] On the other hand, using a multiple antenna configuration, the position of the probe can be estimated with sub-meter accuracy.[10] Both assumptions represent conservative values and better values can be expected for ranging accuracy. Nevertheless, the presented maneuvers are based on these values due to the criticality of this mission phase. Table 1 displays the expected timeline for those operations.

	Distance to target [m]	**Time to capture**
Target approach	>3500	
Initiation of scanning flight sequence	3500	t - 8.5h
Detection of target	3000 - 2000	t - 6h
Target scanning*	1000 - 75	t - 5.2h
Decision GO / NO-GO Capturing	75 - 37.5	t - 15min
First ejection of magnets	75 - 37.5	t - 14min
Second ejection of magnets	37.5 - 75	t - 183s
Connection established	0	t = 0
Magnet retraction	0	t + 20s
Rotation stop	0	t + 180s
Sail deployment	0	

Table 1: Timeline for capturing operations

The first priority during the proximity covered by the near approach and capturing has to be collision avoidance. Therefore a stepwise approach and capturing process is proposed, which is based on repetitive target observations and continuous refinements of target observations. The evaluation of the near approach maneuver is based on sequential converging rotations in v-, h- and r-bar, based on the evaluation of the Clohessy-Wiltshire equations for relative maneuvering. To avoid a possible collision between probe and target, the probe leaves the far approach at a distance of 3500 meters from the expected target location. At this point, the near approach maneuver is initiated by thrusting vertical to the orbital plane. The utilized property of this maneuver is its passive safety since it initiates a rotation around the target, which is periodically performed without closing into the target (neglecting disturbing forces). It is expected, that the target can not be detected instantaneously. This is addressed by performing firings, when the probe is crossing the orbital plane again to tighten the elliptic path around the target, here with a proximity of 500 meters per burn (see figure 4). When the target has been initially detected by the probe's RADAR at approximately 3000 meters, a coordinated flight sequence is started. This involves the transfer between a total of three stable flight levels around the target (compare figure

5). It is constantly intended to keep the target in the center of these flight levels. As measurements become more precise when closing in towards the target, each transfer between two flight levels allows the readjustment of the trajectory with respect to the target. The flight levels around the target and their distance are therefore set to meet the operational ranges of different remote sensing sensors and support a stepwise generation of a precise model of target geometry and motion.

In the displayed trajectory the outer flight level equals the distance of 3000 meters at which the target is detected. The second flight level closes into a base distance of 1000 meters to the target. The natural eccentricity of the trajectory already leads to a minimal distance of under 500 meters to the target. During this fly-by target measurements, observations with increased precision are being conducted to refine the target motion to a level of precision, which allows a risk-free transfer to the third flight level. It has a base distance of 300 meters and closes into approximately 150 meters to the target at the closest point. After a first scan by the LIDAR from this distance, a transfer to the closest flight level at a semi-major axis of 75 meters and a closest proximity of 37.5 meters to the target.

Figure 5 shows the different flight levels and exemplary transfer trajectories, projected into a 2D-plane. In reality, the different flight levels are not planar, but by thrusting in h-bar inclined towards each other. The inclination between two surroundings on the last flight level is set to 45 degrees and the inclination between flight levels one and three is quantified as 90 degrees (compare figure 4). This brings the benefit, that the probe can observe the target from each view angle, independent from the target motion. This introduces maximum precision to the generation of the target model to evaluate the optimal capturing configuration. At a distance of 100 meters from the target, the probe passes the critical point on the trajectory from which its capturing mechanism becomes capable to capture the target.

Of special interest are the periods of the revolutions around the target. This value grows with orbit height, but not with the distance from the target. Thus, the different revolutions need the same time on constant orbit height. Additionally, the period is equal to the period of the revolution of the target around the earth. The minimum relevant period time is approximately 92 minutes at an orbit height of 300 km.

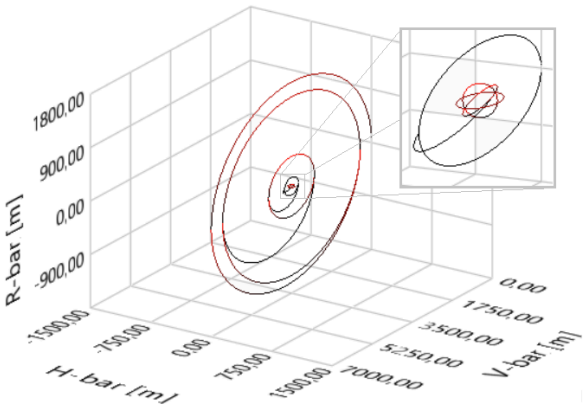

Figure 4: Near approach trajectory in LOF, considering instantaneous burns

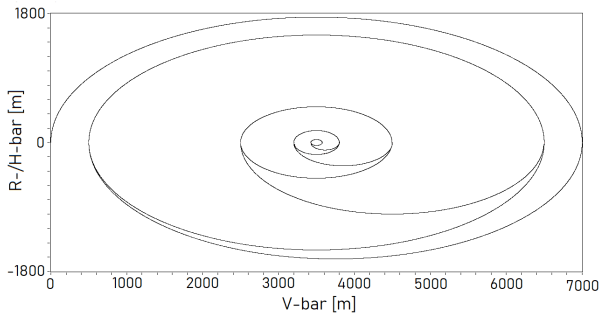

Figure 5: Near approach trajectory in LOF, H-bar and R-bar are projected in one dimension

It is to note that the described flight strategy is completely based on inherent stable motions instead of forced motion flight maneuvers. This requires thrustings only to be necessary at designated points on the trajectory instead of requiring continuous thrusting to follow a trajectory. This does not only require less propellant, but it also allows a much safer flight procedure because the probe itself will remain on certain flight levels, in case a burn is not performed or communication is lost. Only if the probe is left on a flight level for a long time, additional burns need to be performed to account for orbit disturbances. Further investigations to quantify the frequency, as well as the required propellant mass are currently being conducted.

As the propellant tanks of the probe are designed to support worst-case flight scenarios, which involve an injection to a low orbit by the rideshare and a high target orbit, during most flights this results in remaining propellant within the probe after capturing. In case it is not intended to decouple the probe short before target reentry to reuse it for a second deorbiting process, all remaining fuel should

be used to serve the mission objective and accelerate the deorbiting process. To accomplish an accelerated deorbit, an active deceleration of the target would be an option, but due to the high mass ratio between target and probe only fractions of meters per second are achievable. As numeric simulations showed, it is more effective to use the remaining fuel for target eccentricity increase. This benefits the deorbit time because the target starts to penetrate the upper layers of the atmosphere earlier compared to an even orbit decrease. As the tether and sail analysis showed, the energy dissipation of the sail is tremendously increasing with an increased atmospheric density, which in return enables high energy dissipations for each pass through the perigee of an affected orbit. Simulations show, that even the eccentricity change of 0.01 can result in a doubled deorbit speed.

After the probe captured the target, tumbling must be prevented.The initial tumbling of the target can be stopped by the probe using its torquers and propulsion system. While the initial tumbling was induced by disturbing environmental influences, during the deorbiting process torque induced by the force vector of the deorbiting device must be considered. This torque becomes non-zero in case the probe is not placed inline of one of the main system axis and the targets CoG. As this precision can not be reliably provided by the capturing mechanism, another solution is needed. Clarifying the existing torques, it is important to differentiate between the torque induced by the probe being of-center and the torque induced by the probe itself, because the force contributions of tether and sail are varying over the orbit height and are not acting onto the same point. To cancel the second moment, generated by the probe itself, a self-stabilizing moment can be introduced by geometrically shaping the sail in a pyramid shape. The effectivity of pyramidic shaped sails for stabilization has been studied in earlier research.[11] To eliminate the off-center moment between probe and target, the effective force vector of the probes deorbiting devices need to point through the common center of mass. To account for inaccuracies of the capturing mechanism, for this purpose the angle between probe and target can be mechanically adjusted in two dimensions to point its force vector through the target CoG. An initial estimation of the targets CoG position, as well as the position of the probe on the target, is provided by the remote sensing, this allows the derivation of initial values for the probes orientation relative to the target. After this orientation is initially trimmed, the probe is capable to observe the remaining rotation. Based on the observed turn rates, a fine adjustment of the orientation can be applied iteratively.

An especially interesting aspect of the described mission planning is the duration of its active operations. Since the near approach and capturing are performed within several hours, combined with LEOP (launch and early operations) and far approach, the capturing objective can be performed within single weeks after launch. After capturing and stabilizing, the deorbit mechanism is passive in nature, due to the self-stabilizing design of the sail. Thus no active operations are necessary to reach the mission objective, which implies low requirements on component lifetime furthermore resulting in a lower system cost.

Remote Sensing

The remote sensing subsystem is solely active during the near approach and capturing. The tasks of the remote sensing subsystem can be sorted into two categories. First, the remote sensing must constantly measure the relative position of the target to allow a collision-free near approach. This is accomplished by constant RADAR tracking of the target. Second, to enable a safe capturing, the kinematic properties of the target must be known. This includes the position, rotation, moment of inertia, center of mass, and shape. Based on this information a position for contact with the target on successful capturing is determined by the ground station. During capturing, the remote sensing subsystem can monitor the compliance of the probe's motion to the expected behavior.

The second category of tasks is algorithmically challenging and needs more sensors. The DEBRIS probe will use cameras and a solid-state LIDAR for target scanning.[12] Whilst the cameras provide visual information at a high angular resolution, the LIDAR delivers accurate depth measurements at a lower angular resolution. During the sun-exposed phase of the orbit (daytime), special care must be taken to prevent direct sunlight on the sensors. This can be ensured by turning the probe using the AOCS. Additionally, the reflective surfaces used in satellite construction combined with shadows can result in high brightness differences which can not be handled by a common camera. Thus additional high-power LEDs will be used to illuminate the target to carry out visual measurements during nighttime. Their light we bundled using collimators to enhance target illumination. As the period of one revolution around the target equals the period of one revolution around the earth, the probe always

sees the same face of the target during nighttime in the worst case of no target rotation. To solve this problem, the probe can change its revolution direction by thrusting at the same height as the target in the opposite direction.

Figure 6: Example of feature vector matching on preliminary artificial data of a slightly rotated satellite. Model © NASA

Onboard the camera images are searched for visual features of the target which can be described using rotation- and scale-invariant feature vectors (compare figure 6).[13] Of the possible feature vectors a subset of k spatially evenly distributed vectors will be chosen. For each vector, the visual features (RGB color information and reflected laser intensity) will be measured. Additionally, the position of the vector over n frames per orbit around the target is determined by the LIDAR. The frames are distributed in a way to cover the target from as many different perspectives as possible. With $k = 1000$ feature vectors of which no more than 50% are observed per frame and a number of $n = 2000$ frames per orbit the produced 26.7MB of data can be transmitted to the ground station in less than 14s assuming a transmission rate of 2MB/s. This enables to stream the observational data to the ground station on each contact. The remaining bandwidth is used to transmit selected camera and LIDAR images allowing the validation of the algorithm on the probe by the ground station.

The ground station aggregates the feature vector movements. Using this data, it can derive the position, rotation, moment of inertia, center of mass and shape of the target.[14,15] This allows for the extrapolation of the targets movement and the detailed planning of a capturing procedure. Using continuous updates from the probe this derived information is iteratively improved until it converges. Due to the stable nature of the near approach flight trajectory, the transmission of the updated feature vector positions is not time-critical. Thus, this method is robust against connection failures.

Whilst the ground station can use almost arbitrarily large computing resources, the probe is limited in this respect. This is tackled by the employment of two concepts: First, the feature detection algorithm can be easily parallelized and can thus use multiple processing units. Second, the use of FPGAs allows for a hardware-optimized algorithm increasing performance and power-efficiency.

To evaluate the setup of the remote sensing subsystem, a dedicated study will be made. As there is no dataset of a similar type to the produced one known to the authors, the approach will be as follows: First, a rendering engine will be developed using a ray-casting technique and physically based rendering to closely match the visual conditions in space. This can be validated using imagery taken in space, e.g. from the ISS. From this point on, artificial camera, RADAR and LIDAR data can be generated for testing. This allows for the evaluation of different processing units, algorithms (feature detection and properties derivation), and resolutions.

As the necessary cameras are lightweight and not too expensive, redundant cameras are used. As long as two cameras spread over one surface of the probe are active, the function of the LIDAR can be replaced using a stereo vision setup. As the necessary feature matching is already part of the algorithm, the switch is computationally inexpensive. However, calculations show that the depth precision of the stereo vision setup will be considerably lower than the measurements of the LIDAR. As depth inaccuracy of a stereo vision setup grows quadratic with the depth itself, the stereo vision system can be used during the parts of the orbit where the probe is nearest to the target. This thus offers a redundant solution for the target scanning in case of LIDAR failure.

Capturing

Generally capturing the target is regarded as one of the most difficult steps in active space debris removal. In earlier approaches different capturing mechanisms where investigated, including the utilization of nets,[16] harpoons[17] and robotic arms.[18] Current investigations favor the use of robotic mechanisms since they provide good controllability and a stiff connection. Even though robotic mechanisms have been taken into consideration for initial trades, they were rated as inappropriate for implementation into a small satellite. Their downside is especially connected to the large required system envelope concerning mass and volume. Also, cases, where the masses of the capturing mechanism and the probe itself are in a similar range, correspond to immense complexity regarding AOCS operations. Even though earlier capturing approaches have also been demonstrated on a small satellite scale, the criticality of the process for mission success combined

with experienced difficulties in previous demonstrations leads to the decision to develop a new capturing approach. To achieve this critical step during mission operation a novel capturing mechanism is proposed. Before the principle of operation is being described, the requirements for the capturing mechanism are summarized:

- The capturing mechanism shall be able to establish a physical connection to the target
- The capturing mechanism shall consume no more than 20 W.
- The capturing mechanism shall have a mass of a maximum of 6 kg.
- The capturing mechanism shall have a maximum volume of 3 U.
- The capturing mechanism shall be capable to perform capturings over a distance of 100 m.
- The capturing mechanism shall be capable to perform at least 5 capturings
- The capturing mechanism shall be capable to disengage already established connections.

The proposed mechanism is based on the ejection of magnetic projectiles, which remain physically connected to the probe by aramid ropes. For the acceleration of the projectiles two principles are currently being investigated, where one is electromagnetic acceleration and the other one uses gas pressure. First calculations show, that both principles are suitable to accelerate the projectile to the intended ejection velocity, which lies in the range of 0.1 to 1 meters per second. Since the projectiles are magnetized, it is possible to aim and influence the trajectory of the projectiles by adjustable electromagnets in front of the projectile outlet while keeping the orientation of the probe constant. The aramid rope is connected to a motor, which enables it to retract already ejected projectiles back into the barrel and control ejection velocity. Due to the orbiting of the probe around the target, the drifting effects induced by this must be taken into account. Optimal usage of the probe's velocity can be made when it is closest to the target at t_1. Therefore, the probe ejects half of the projectiles at t_0 missing the target on the one side. At t_2 the second half is ejected to miss the target on the other side. When the magnets meet and connect a physical connection is created and each pair of separately ejected aramid ropes now form a loop around the target. Due to a careful choice of the times and angles of ejection, the distance between the projectiles can be minimized such that they only need to compensate for the ejection precision. Experimental values show a feasible precision requirement of 0.5° for projectiles with a mass of 4g. The probe currently contains 12 projectiles, which enables it to create 6 loops around a given target (t_3).

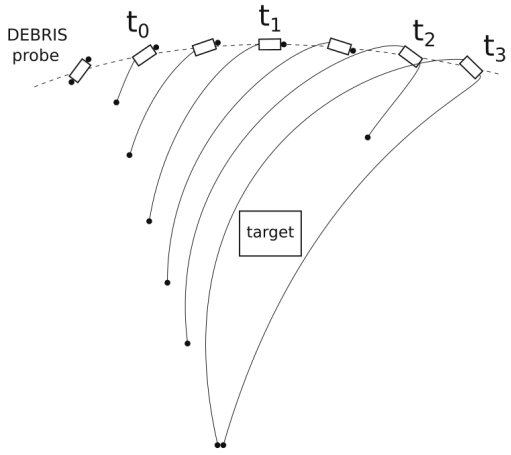

Figure 7: Two-dimensional trajectory of magnetic projectiles after ejection

From this point on, the probe will begin to retract the aramid rope, tightening the loop around the target. Ultimately this leads to tie the target to the probe and establish a physical connection. One major advantage is the possibility to open established connections again or restart a capturing maneuver, in case an initial approach was not successful. Therefore the included motors need to provide enough torque to separate both magnets. Additionally, the probe can be steered towards a specific place on the target by controlling the torque of the motors utilizing measurements by the remote sensing subsystem. This can be used to target a place where the later deorbit force is in line with the CoG to give an initial configuration for further optimization. For future development, a registration for a patent is currently being conducted.

To demonstrate the feasibility of this capturing approach, a numerical simulation has been implemented with the DART[19] physics engine. Therefore, the probe is assumed to maintain its orbit and orientation towards the target using its AOCS on a worst-case orbit of 2000km height. The magnets are simulated using a dipole-dipole-model.[20] The rope is approximated by a set of cylindrical segments with ball joints in between. A small dampening had to be introduced to account for numerical instabilities. This resembles small frictions inside the rope. Using this simulation, it could be shown, that the capturing mechanism completes successfully in 17 minutes. The rope positions and projectile trajectories can be seen in figure 7.

Satellitebus

Propulsion Regarding its propulsion subsystem, the main requirements from the mission profile are the necessity of two very different thrust levels for transfer and relative flight, as well as the ability to perform quasi-instantaneous thrustings, especially at low impulse changes. To meet these requirements a chemical propulsion system was designed, based on green bi-propellant thrusters. The system is backed by a high volume propellant tank to provide a high Δv-capability and lower the requirement regarding orbit injection by the launcher. To achieve both low and high thrust requirements at adequate impulse bits an architecture with two sets of thrusters is realized. On the one hand, a 22N-thruster is implemented as the main engine, the second side of the system is realized by using sets of COTS cubesat thrusters at 0.5N thrust for high accuracy maneuvers. Both engine types provide a specific impulse of 285 seconds. To reduce piping and supply tanks all available thrusters use the same propellant and are fed by the same propellant tanks.

	No.	Δv **[m/s]**	ΔI **[Ns]**
LEOP	1	139.3	5572
Far approach	1	659.8	26392
Stationkeeping	1	35.6	1424
Margin transfer	10%	83.47	3338.8
Near approach	10	46.6	188
Margin n. a.	20%	9.4	376
Total		**974.57**	**38982.8**

Table 2: Summarized propulsion budget

Table 2 gives an overview of the propulsion budget and the required capabilities. The relatively high value for propulsion operation in LEOP is caused by the included capability to reach a parking orbit before its further operations. Quantitative values were obtained for a situation where the probe is injected into a 350km orbit by the rideshare and establishes a 600km parking orbit during LEOP. The budgeted far approach capability is based on a worst-case scenario, where the probe needs to achieve the upper bound of the investigated 2000km LEO region. To maintain the correct orbit and perform fine adjustments to match with the target orbit, an additional 35.6 $\frac{\mathrm{m}}{\mathrm{s}}$ were accounted for stationkeeping. Up to this point, all positions of the budget are part of the transfer, to this subbudget a margin of 10 % is assigned to account for slight course variations and losses in engine and propulsion operations. Since all values are calculated for the worst-case scenario a probe is only capable to perform this maneuver in once in a worst-case scenario.

The near approach and capturing require much smaller orbit corrections, but have a much higher criticality concerning timing and precision, this is the reason why ten attempts are foreseen in the propellant budget and their margin is increased to 20%.

Due to shared supplies, in the worst case of a main engine failure, the auxiliary engines can excess all available propellant resources and work as a backup propulsion system. Of course, in this case, the loss of thrust will increase finite burn losses. But even taking these into account the initially designed large Δv-capability of the system will still provide enough reserve to enable the transfer to secondary space debris targets. It, therefore, is important to note, that even a main engine failure will not necessarily lead to a loss of mission.

AOCS The requirements regarding the Attitude and Orbit Control System (AOCS) are similar to other small satellite missions, especially requirements regarding turn rates and accuracies are moderate. This enables the purchase of system components from suppliers to reduce development effort. The AOCS is based on an extended IMU, which is fed by visual feedback from navigation cameras which effectively function as earth sensors. Additional sensory input is given by sun sensors and an absolute position reference is provided by a differential GNSS receiver. Fine requirements exist concerning the target at the capturing process, which is covered by an additional designated sensor set. The most interesting aspect of the AOCS is attitude determination during the capturing phase, which happens close to the target. In this phase, it is not the common attitude with respect to earth and sun, which is required, but the attitude with regard to the target center and the sun. When entering the near approach and relative navigation, therefore also information of the remote sensing system is fed into the AOCS algorithms, introducing a new reference point at the target's center of gravity. Since the system is operated in LEO, it is possible to use magnetorquers as actuators. This especially suitable along the systems x- and y-axis, since the architecture already includes electromagnets, which are oriented exactly along this direction. They were initially included to provide the functionality to the capturing mechanism, but are now also shared as actuators for the AOCS. In case of strong tumbling, also the auxiliary thrusters of the propulsion system are capable to introduce torque into the system to assist a detumbling process.

Structure The integrity of the system is provided by a metal frame. In favor of good manufacturability, it is made from a space-proven aluminum alloy Al-7075. Since induction processes would be an issue near the capturing mechanism, parts without significant structural requirements in this area are manufactured from hybrid carbon fiber reinforced plastic. Although the outer dimensions of the probe are beyond the cubesat standard, sections of its frame include the standardized mounting points to include cubesat components that can still be integrated into the probe.

Communications The communications subsystem is responsible to establish and hold a data link with the required bandwidth. The subsystem contains two different sets of transmitters, from which one is operating in X-band and one is operating in S-band. Both transmitters are connected to a row of antennas. Both transmitters, as well as the antennas, are COTS hardware normally used within the cubesat sector. The required bandwidth of the different subsystems strongly varies with mission phases. Especially during capturing the remote sensing generates a significant portion of the entire data stream. This data stream is transmitted towards the ground station to enable sufficient monitoring of the capturing process. Besides the capturing mechanism, the remote sensing and the data from experimental modules, the remaining data streams are due to housekeeping and state monitoring of the probe. In total the required bandwidth peaks during capturing, which therefore is again the mission phase with the most ambitious requirement for the subsystem. The monitoring of the experimental components is identified as a high priority data stream during deorbit since the temporal development of the experimental components over the long deorbit phase is a major contribution to the scientific part of the mission and future technological advancements to the DEBRIS probe and its spin-offs. Referring to available components, the S-band connection will be low bandwidth and supports 9600 baud per second, where the X-band connection can support up to 20 Mbit per second in case sufficient ground contact is given. The main advantage of the S-band system is its omnidirectional antenna characteristic, but the high bandwidth connection requires the correct orientation of the probe. The low bandwidth connection is suited to transmit the housekeeping data, while the X-band connection is mainly required during the capturing. Besides housekeeping, the functional usage of the S-band connection is also especially interesting for system recovery.

Although the system layout does not change after capturing, the contact times change significantly. Two different influences need to be respected: on the one hand the physical influence of the now captured target as well as the deployed sail. For the calculation of contact times, the contact time to the X-band transmitter is therefore expected to be reduced to 50% after capturing. It is probable, that the antenna characteristic of the S-band connection is less affected after capturing since its propagation is only expected to be blocked by the target body, but other than the X-band propagation, not by the sail structure. Reflecting on the mission profile and occurring data streams, this is acceptable, since the effective bandwidth requirement drops substantially after capturing. The highest data loads are generated by the experimental modules and the state-monitoring of COTS components, but both of these data types do not have real-time requirements. This enables a buffering within the onboard storage and transmitting them via X-band as soon as ground contact is established.

Conclusion and Next Steps

DEBRIS Technology Demonstrator I

The next major step on the roadmap towards the DEBRIS probe will be the development and operation of DETECTOR I (DEbris TECnology demonstraTOR I). This demonstration mission on a cubesat scale will provide flight heritage to critical components and set the stage for the first DEBRIS active removal mission. The primary mission objective of DETECTOR I is to detect a debris object in space and conduct observations about its motion and tumbling.

This includes several secondary objectives and requirements for critical subsystems. Since DEBRIS heavily relies on COTS components to meet its cost requirements, DETECTOR I will not only be a demonstration, but also an evaluation mission. Since many of the used systems do not have flight heritage and no present experience about their behavior in the space environment, the payload consists of several testbeds to evaluate these parameters under an operational environment.

Besides the technological aspects, DETECTOR I will also provide insight and knowledge regarding processes and operations. Especially the flight procedures will be similar to the proposed flight profile for the DEBRIS mission. After the completion of its primary mission, DETECTOR I includes its own tether and sail to deorbit itself. This last step in

its mission will provide viable data for those devices deorbiting characteristics, which will enable further verification of the numerical simulations. During the deorbit phase, the time until reentry will be used to measure the degradation of the experimental components.

To support the future development of the DEBRIS mission, extra co-workers and capital will be needed. Thus, a startup will be founded which will steer the DEBRIS mission to successful launches.

Scientific Merit & Industry Relevance

Scientific merit Besides DEBRIS' function as an active debris removal vehicle, it also acts as a flying testbed for newly developed modules in support of agile development philosophy. Not only the use of COTS components in the design but also the included experimental modules support the investigation of the interaction between components initially designed for other applications and the space environment. It therefore strongly supports current new space approaches. As an addition to its testbed function, the DEBRIS Probe will especially serve a scientific purpose regarding the generation of new data in the fields of space debris properties, propagation, development, and the space debris environment. Current databases are created using observations based on ground radar observations, which are strongly affected by atmospheric disturbances and are containing many uncertainties.[21] Since a DEBRIS probe after capturing enables the active observation of a deorbit trajectory, the uncertainties within its measurements will be much lower. It is therefore also possible to observe the trajectory of debris objects with attached probes with much higher precision. This will allow better differentiate influences of gravitational, atmospheric, and electromagnetic effects on the trajectory. This increased knowledge can then be used to refine the known space debris models and databases to better understand its future development and be able to fly more precise collision avoidance maneuvers. The created database can within scientific analysis also be used to model or verify gravitational obliqueness, as well as the orbital atmospheric and electromagnetic environment.

Industry Relevance The space debris situation and its possible future propagation pose a critical threat to all current and future satellites. Possible consequences are the loss of spacecrafts and their associated ground services, increasing the risk for industry, government, and the earth's society over time.

Therefore already several projects worked on active debris removal systems, where each of them to this date focused on technology demonstration but did not consider its cost-wise scalability. Taking into account the large number of debris objects in orbit, the deorbiting cost per object has to be reduced well below a million dollars per mission to create an imaginable scenario. The DEBRIS probe is an effective deorbiting device for the whole LEO region, which realizes all required capabilities in a minimal system envelope. Further cost reductions are achieved by heavily relying on the use of COTS components. Additionally, the reduction of launch cost is addressed, by designing the probe in a way that five DEBRIS probes can be deployed together, occupying exactly one ESPA slot.

With the development of the DEBRIS probe contributions are made to key technologies for various new space activities. The relative maneuvering phase contains important methods to tackle problems like target scanning, establishing a physical connection, and flight approach planning. This does not only extend to the fields of satellite inspection and active debris removal: Research into on-orbit servicing tasks like refueling or repairing will highly profit from the knowledge that can be obtained while developing, testing, and sending the DEBRIS probe to space.

On authority level, space legislation heavily discusses the question of liability for inoperative satellites, constantly evaluating to make their earlier operators liable for possible damages in space or on ground.[22] A legislative change in that direction would create tremendous capital risk for satellite operators, creating possible fees in the magnitude of several hundred million dollars for orbital collisions with an operative spacecraft. The DEBRIS probe is a small satellite alternative to prevent this scenario. It offers a solution to remove debris and therefore the risk for the operators, at a more than competitive price for the industry.

As a society, action must be taken now to cope with the debris problem, or space operations will render impossible in the near future. The global community needs a plan for active debris removal to ensure the safe and sustainable operations of the satellites our society relies on. The DEBRIS mission is a contribution to the solution of this important problem.

References

[1] D. J. Kessler and B. G. Cour-Palais. Collision frequency of artificial satellites: The creation of a debris belt. *Journal of Geophysical Research*, 83:2637–2646, 06 1978.

[2] D. J. Kessler. Collisional cascading: The limits of population growth in low earth orbit. *Advances in Space Research*, 11:62–66, 1991.

[3] G. Bonin, J. Hiemstra, T. Sears, and R. E. Zee. The canx-7 drag sail demonstration mission: Enabling environmental stewardship for nano- and microsatellites. *Proceedings of the 27th AIAA/USU Conference*, 2013.

[4] H. Klinkrad, J.R. Alacon, and N. Sanches. Collision avoidance for operational esa satellites. *Proceedings of the Fourth European Conference on Space Debris*, 04 2005.

[5] USSTRATCOM (U.S. government). Satcat data portal. `https://space-track.org`. Accessed: 2020-01-25.

[6] ESA. Discos data portal. `https://discosweb.esoc.esa.int`. Accessed: 2020-01-25.

[7] J. Ellis and C. Hall. Model development and code verification for simulation of electrodynamic tether system. *Journal of Guidance Control and Dynamics - J GUID CONTROL DYNAM*, 32:1713–1722, 11 2009.

[8] B. Cotten, I. Bennett, and R. E. Zee. On-orbit results from the canx-7 drag sail deorbit mission. *Proceedings of the 31st Annual AIAA/USUConference on Small Satellites*, 08 2017.

[9] C. Jianrong and L. Junfeng. Analysis of orbit accuracy for non-cooperative earth-orbiting objects. *Open Astronomy*, 28:191–199, 12 2019.

[10] D. Kuang, W. Bertiger, S. Desai, and B. Haines. Precise orbit determination for leo satellites using gnss tracking data from multiple antennas. In *23rd International Technical Meeting of the Satellite Division of the Institute of Navigation 2010, ION GNSS 2010*, volume 4, 09 2010.

[11] N. Miguel and C. Colombo. Deorbiting spacecraft with passively stabilised attitude using a simplified quasi-rhombic-pyramid sail. *Advances in Space Research*, 2020.

[12] B. A. Sornsin, B. W. Short, T. N. Bourbeau, and M. J. Dahlin. Global shutter solid state flash lidar for spacecraft navigation and docking applications. In *Proceedings of SPIE vol. 11005*, 2019.

[13] D. G. Lowe. Distinctive image features from scale-invariant keypoints. *International Journal of Computer Vision*, 60(2), 2004.

[14] B. E. Tweddle, A. Saenz-Otero, J. J. Leonard, and D. W. Miller. Factor graph modeling of rigid-body dynamics for localization, mapping, and parameter estimation of a spinning object in space. *Journal of Field Robotics*, 32(6), 2015.

[15] B. Tweddle. Computer vision-based localization and mapping of an unknown, uncooperative and spinning target for spacecraft proximity operations. *Doctoral Thesis*, 2014.

[16] U. Battista and A. Landini et. al. Design of net ejector for space debris capturing. In *Proceedings of the 7th European Conference on Space Debris*, 2017.

[17] R. Dudziak, S. Tuttle, and S. Barraclough. Harpoon technology development for the active removal of space debris. *Advances in Space Research*, 16, 04 2015.

[18] S. Nishida, D. Uenaka, R. Matsumoto, and S. Nakatani. Lightweight robot arm for capturing large space debris. *J. of Electrical Engineering*, 6, 09 2018.

[19] J. Lee, M.X. Grey, S. Ha, T. Kunz, S. Jain, Y. Ye, S.S. Srinivasa, M. Stilman, and C.K. Liu. DART: Dynamic animation and robotics toolkit. *The Journal of Open Source Software*, 3(22):500, February 2018.

[20] K.W. Yung, P.B. Landecker, and D.D. Villani. An analytic solution for the force between two magnetic dipoles. *Magnetic and Electrical Separation*, 9(1):39–52, 1998.

[21] M. Weigel and A. Patyuchenko. Orbit determination error analysis for a future space debris tracking radar. *Proceedings of the European Space Surveillance Conference*, 06 2011.

[22] J. A. Dennerley. State Liability for Space Object Collisions: The Proper Interpretation of 'Fault' for the Purposes of International Space Law. *European Journal of International Law*, 29(1):281–301, 05 2018.